

Fitting studies in δm^2 vs $\sin^2 2\theta$ space

Rajendran Raja

20-Nov-1999

We describe preliminary results obtained by fitting for δm^2 and $\sin^2 2\theta$ using simulated data from a muon storage ring. The simulated histograms were provided by Stephen Geer using a program incorporating a 3 neutrino oscillation scheme and matter effects. We have setup a fitting scheme that uses interactive MINUIT .

The Method

The first set of fitting data, denoted as Set 1, is from a simulation of a muon storage ring with the following characteristics. The characteristics of the oscillation scenario are shown in table I and the values chosen correspond to the scenario IA1, the so-called large mixing angle solar MSW solution that can be found at http://www.fnal.gov/projects/muon_collider/nu_study/parameters.html. For this scenario we choose various values of the muon storage ring momentum and distance to the detector, which are characterized as sets numbered from 1 to 8 and estimate the errors for each set.

The amplitude for muon neutrino disappearance can be written as

$P(\nu_\mu \rightarrow \nu_\tau) = \cos^4 \theta_{31} \sin^2 2\theta_{32} \sin^2(1.267 \delta m_{32}^2 L / E_\nu) = A \sin^2(1.267 \delta m_{32}^2 L / E_\nu)$, where the amplitude A is given by $\cos^4 \theta_{31} \sin^2 2\theta_{32}$ and is equal to 0.9216 for scenario IA1 central value. The survival probability $P(\nu_\mu \rightarrow \nu_\mu)$ is then given by $(1 - P(\nu_\mu \rightarrow \nu_\tau))$. Matter effects were generated for the given baseline length of 2800 km assuming $\delta m_{32}^2 = m_3^2 - m_2^2 > 0$ and $\delta m_{21}^2 = m_2^2 - m_1^2 > 0$. If E_{true} is the true neutrino energy, and E_{obs} the observed neutrino energy, (taken as the sum of the muon and hadronic final state measured energies), then the observed energy spectrum is given by

$$\frac{dN}{dE_{obs}} = \int dE_{true} P(E_{obs} | E_{true}) \frac{dN}{dE_{true}} (1 - \cos^4 \theta_{31} \sin^2 2\theta_{32} \sin^2(1.267 \delta m_{32}^2 L / E_{true}))$$

where $P(E_{obs} | E_{true})$ is the (cross section*detector smearing function) probability of observing the energy E_{obs} given a true neutrino energy E_{true} . This can be re-written as

$$\begin{aligned} \frac{dN}{dE_{obs}} &= \int dE_{true} P(E_{obs} | E_{true}) \frac{dN}{dE_{true}} \\ &- \cos^4 \theta_{31} \sin^2 2\theta_{32} \int dE_{true} \frac{dN}{dE_{true}} P(E_{obs} | E_{true}) \sin^2(1.267 \delta m_{32}^2 L / E_{true}) \end{aligned}$$

The first term on the right hand side is the neutrino spectrum that would be observed in the absence of oscillations. The second term is the *unobserved* spectrum due to oscillations. Notice that the mixing angle terms act as a scaling factor for the unobserved part. The effect of the mixing angle can be simulated by working out the unobserved spectrum for a particular value of the mixing angle and scaling this to other values.

Generation of the template distributions

Stephen Geer has generated histograms for the above scenario, varying δm_{32}^2 from 0.0025 to 0.0045 eV^2/c^4 . The “neutrino energy” plotted is defined as the energy of the observed muon and the hadronic final state smeared by realistic detector resolutions. These histograms (four of them) are shown in Figure 1.

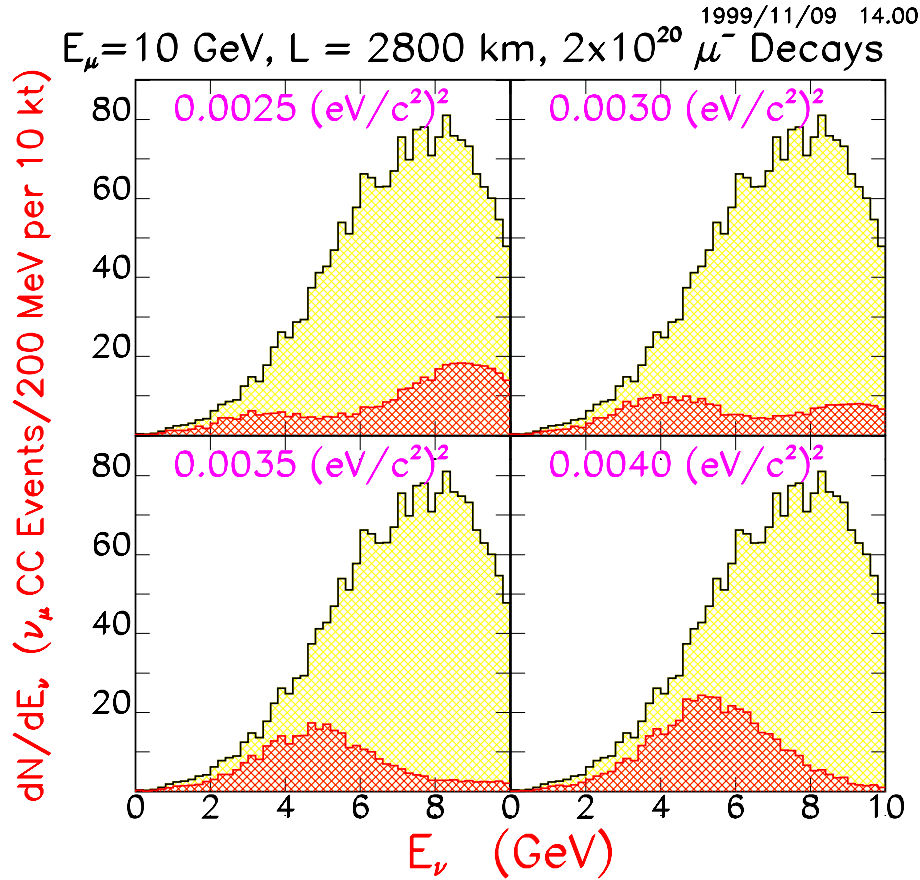


Figure 1 Oscillated and non-oscillated spectra for scenario IA1 for various values of δm_{32}^2 .

We have read the 5 oscillated histograms (for the 5 values of δm_{32}^2) and the unoscillated histogram into the fitting program and worked out the unobserved spectrum for each value of δm_{32}^2 . We have interpolated the unobserved histograms bin by energy bin for any value of δm_{32}^2 using Newton's divided difference polynomial interpolation formula. Thus it is possible to generate theoretical expected energy distributions for any arbitrary value of $\sin^2 2\theta_{32}$ and δm_{32}^2 . For this study, we leave θ_{31} fixed ($\sin^2 2\theta_{31} = 0.04$) so that $\cos^4 \theta_{31} = 0.97989$. We can also generate experimental distributions for a particular value of $\sin^2 2\theta_{32}$, δm_{32}^2 by generating the theoretical spectrum for that point and then generating the experimental distribution for the expected number of events using the HBOOK routine HRNDM1 on the theoretical distribution. This will thus simulate the appropriate

statistical fluctuations in the experimental distribution that is consistent with the expected statistics. These fluctuations are of course absent in the theoretical template.

Likelihood function

We use MINUIT to fit for a given generated experimental distribution by minimizing a negative log-likelihood function Λ given by the following formula.

$$\Lambda = -\sum_{i=1}^{i=nevents} \log_e P_i^{theor} + \frac{(N_{exp} - N_{theor})^2}{2N_{exp}}$$

For each event, P_i^{theor} gives the probability of observing the event with its neutrino energy obtained by normalizing the theoretical distribution to 1. The second term gives the likelihood of the theoretically expected number of events fluctuating to the experimentally observed number. After minimization, 1σ , 2σ and 3σ contours are evaluated in $\sin^2 2\theta_{32}$, δm_{32}^2 space by requiring that the negative log likelihood changes from the minimum by 0.5, 1.0 and 1.5 units. When the statistics of the observed events exceeds a settable minimum (20,000 events), we switch to a binned likelihood function evaluated as

$$\Lambda_{binned} = \sum_i^{nbins} (N_{exp}^i - N_{theor}^i)^2 / (2N_{exp})$$

which is the usual expression for $\chi^2/2$.

Results

For each set, we have studied 10 points in $\sin^2 2\theta_{32}$, δm_{32}^2 space and plotted the contours. Significant correlations are observed between the errors in $\sin^2 2\theta_{32}$ and δm_{32}^2 . These contours can be seen in Figures 2 for set 1. Figures 3-10 show the contours for sets 2-9. Figures 11-19 show the experimental and fitted distributions for the 10 points under study for set 1 to set 9. It was necessary to limit the fitted events to the low energy bins especially for Sets 3, 6 and 8, the 732 km points that have large statistics and low sensitivity. The colored hatched area in the figures 11-19 show the bins that are used for the fit. The errors in the fits can be understood as follows. Let us approximate the incoming neutrino flux by a delta function of energy = $E_{average} \sim 7\text{GeV}$, and also assume no smearing. Then the observed number of events can be written

$$N_{obs} = N(1 - \sin^2 2\theta \sin^2(1.267\delta m^2 L / E_{average})) = N(1 - xy), \text{ where } x = \sin^2 2\theta \text{ and } y = \sin^2(1.267\delta m^2 L / E_{average}).$$

Then $\frac{\partial N_{obs}}{\partial x} = -Ny$ and $\frac{\partial N_{obs}}{\partial y} = -Nx$. If one assumes that the shape of the distribution does not change

significantly in the neighborhood of the medium, the standard error σ_x in x is related to ϵ_x , the amount one has to move in x such that the number of observed events change by one standard deviation, i.e. $\sqrt{N_{obs}}$. This yields,

$$\epsilon_x = \frac{\sqrt{1-xy}}{\sqrt{Ny}} \text{ and } \epsilon_y = \frac{\sqrt{1-xy}}{\sqrt{Nx}}. \text{ The error in } \delta m^2 \text{ is given by } \epsilon_{\delta m^2} = \frac{\epsilon_y}{2\lambda \sin(\lambda \delta m^2) \cos(\lambda \delta m^2)}, \text{ where}$$

$\lambda = 1.267L/E$. At resonance, $y=1$ and with strong mixing, $x=1$, so both ϵ_x and ϵ_y are zero. However, at

resonance, $\lambda \delta m^2$ is at $\pi/2$, so $\cos(\lambda \delta m^2)$ is close to zero. For $x=1$, this yields $\epsilon_{\delta m^2} = \frac{1}{2\lambda \sqrt{N}}$ i.e. a finite error

(due to the Jacobian) which decreases with \sqrt{N} . The error in $\sin^2 2\theta$ is however zero at resonance. This implies that once we know the approximate values of $\sin^2 2\theta$ and δm^2 , one can tune the energy of the ring to put that spot close to resonance and produce minimum fitting errors in the parameters. Note that the above formulas for error are approximate but tell us a great deal about the behavior of the fitting errors.

Table 1 Muon Storage ring and oscillation scenario parameters

Parameter		Value	
Muon flux		2x10 ²⁰ decays/year	
Detector fiducial exposure		10 kiloton-years	
δm_{32}^2 values		0.0025,0.0030,0.0035,0.0040,0.0045 eV ² /c ⁴	
δm_{21}^2		5.0 x 10 ⁻⁵ eV ² /c ⁴	
δm_{31}^2		3.5 x 10 ⁻³ eV ² /c ⁴	
$\sin^2(2\theta_{12})$		0.18	
$\sin^2(2\theta_{23})$		1.0	
$\sin^2(2\theta_{31})$		0.04	
δ (CP violating phase)		0.0	
Set number	Muon momentum GeV/c	Distance ring to detector (km)	Fitting energy range GeV
Set 1	10.0	2800.	0-10
Set 2	30.0	2800.	0-12
Set 3	30.0	732.	0-12
Set 4	30.0	7332.	0-25
Set 5	50.0	2800.	0-10
Set 6	50.0	732.	0-12
Set 7	50.0	7332.	0-28
Set 8	10.0	732.	0-4
Set 9	10.0	7332.	0-12

Preliminary Conclusions

The best error values are flagged by arrows in the tables. The least error seems to occur for Set 1 (10Gev,2800km) point 8, Set 2 (30 GeV 2800km) point 9, Set 4(30GeV 7332km) points 7,8,9 , and Set7(50GeV 7332km) points 7,8,9 . One may conclude that the fitting method under study here does poorly for the 732km scenario, where one is overwhelmed by the unoscillated neutrino spectrum.

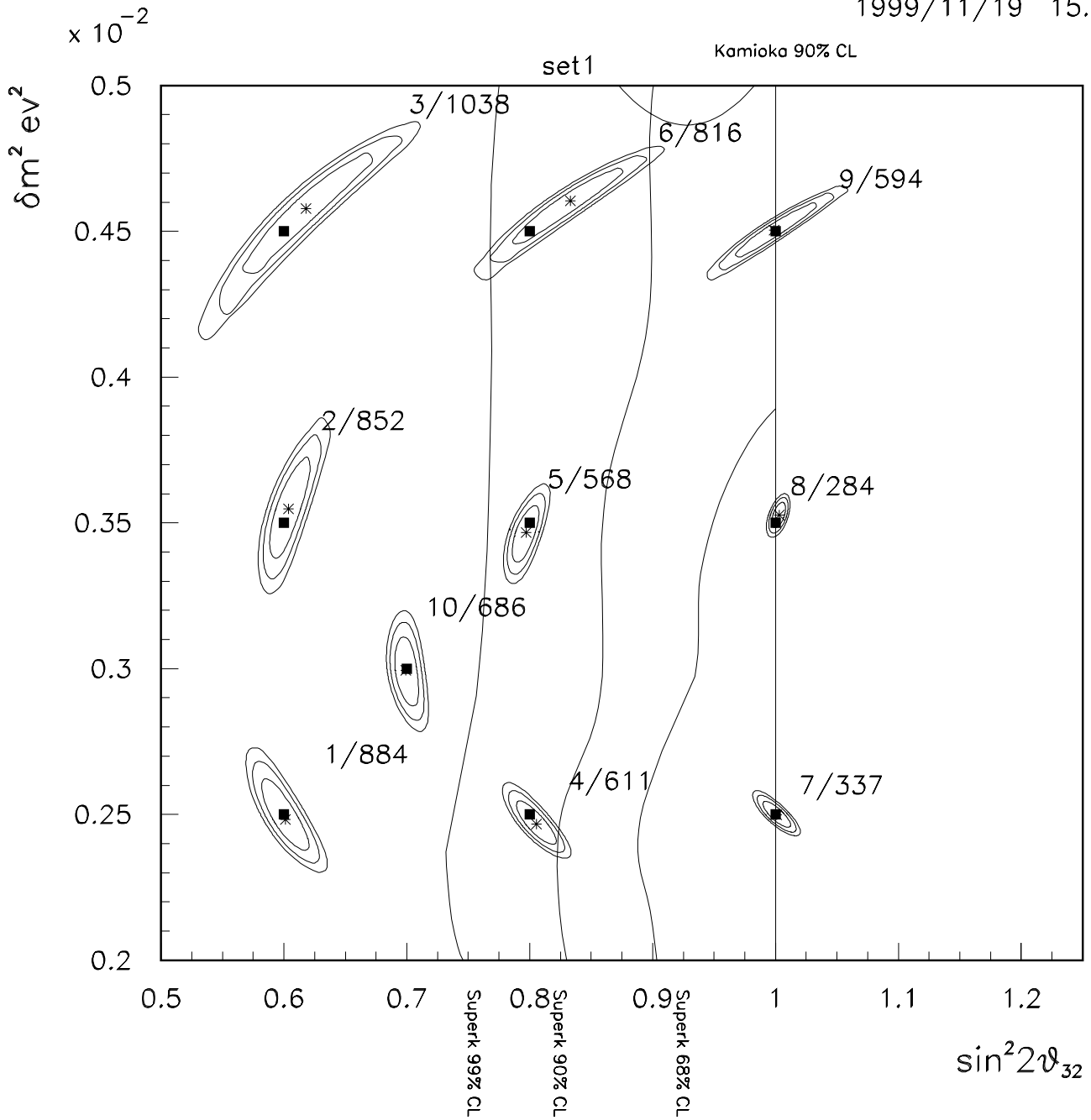


Figure 2 Set 1- Error contours for 10 experimental points, at likelihood intervals of 0.5,1.0 and 1.5 corresponding to Gaussian 1σ , 1.4σ and 1.7σ respectively. The dark rectangles denote the generated points and the *'s show the fitted points. Fitting sequence numbers and the number of events at each point are shown . For instance 7/337 means point 7 with 337 events. SuperKamioka and Kamioka atmospheric error contours may be seen superimposed.

Table 2 shows the results of the fit for set 1. The 10 fitted point co-ordinates are given, together with the 1σ errors and the percentage errors for the co-ordinates. Point 8 is close to resonance for this set and gives the minimum percentage errors of 1.12% and 2.44% for $\sin^2 2\theta$ and δm^2 respectively. As one goes away from the resonance, errors increase. Tables 3-10 show the results for sets 2-9. General conclusion to be drawn- 732 km points are hard to fit and give bad errors with the current technique, despite the large statistics. Table 11 shows a summary for all sets for the canonical point $\sin^2 2\theta$, $\delta m^2 = 1.0, 0.35 \times 10^{-2} \text{ eV}^2/\text{c}^4$.

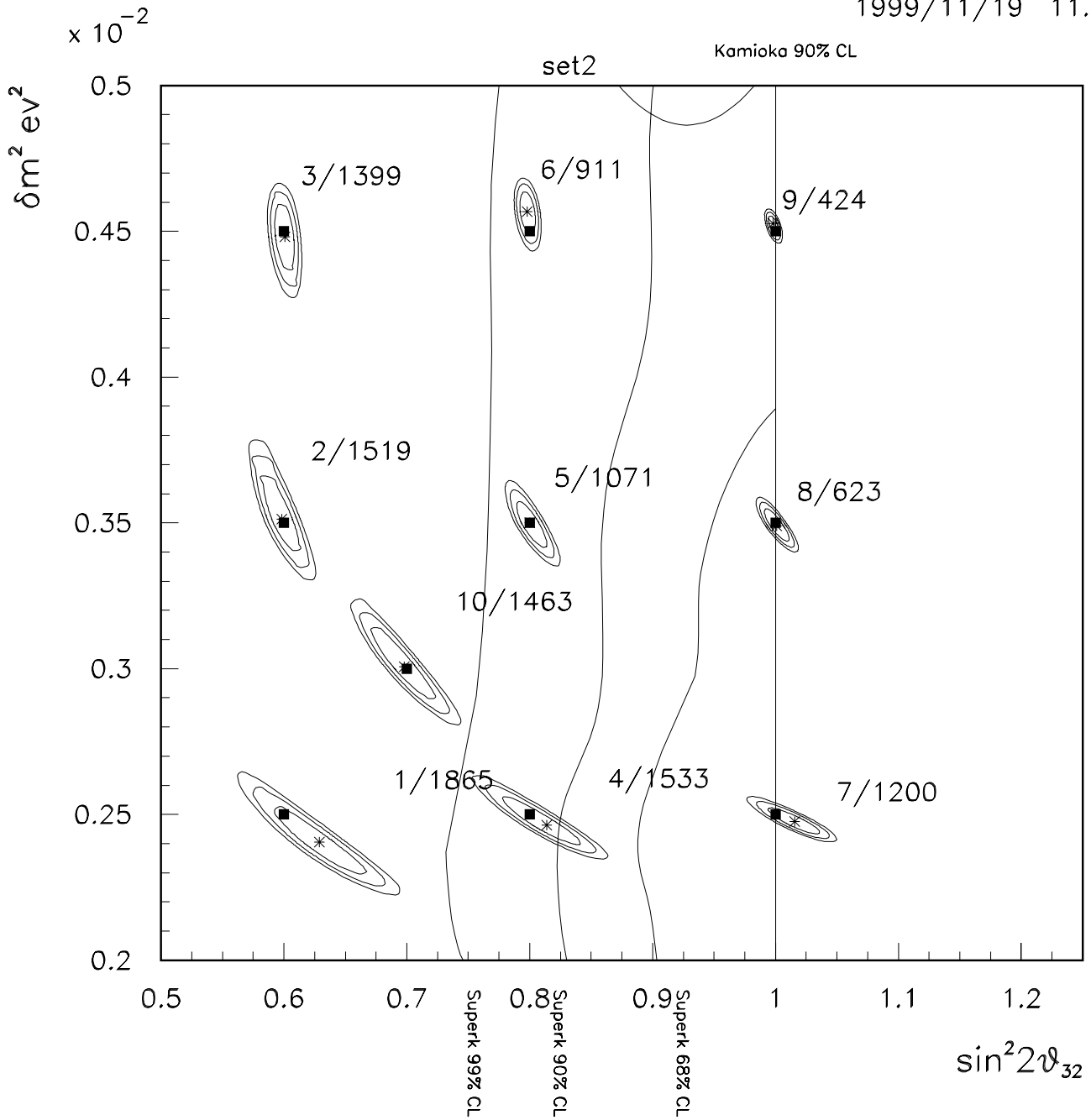


Figure 3 Set 2- Error contours for 10 experimental points, at likelihood intervals of 0.5,1.0 and 1.5 corresponding to Gaussian 1σ , 1.4σ and 1.7σ respectively. The dark rectangles denote the generated points and the *'s show the fitted points. Fitting sequence numbers and the number of events at each point are shown . SuperKamioka and Kamioka atmospheric error contours may be seen superimposed.

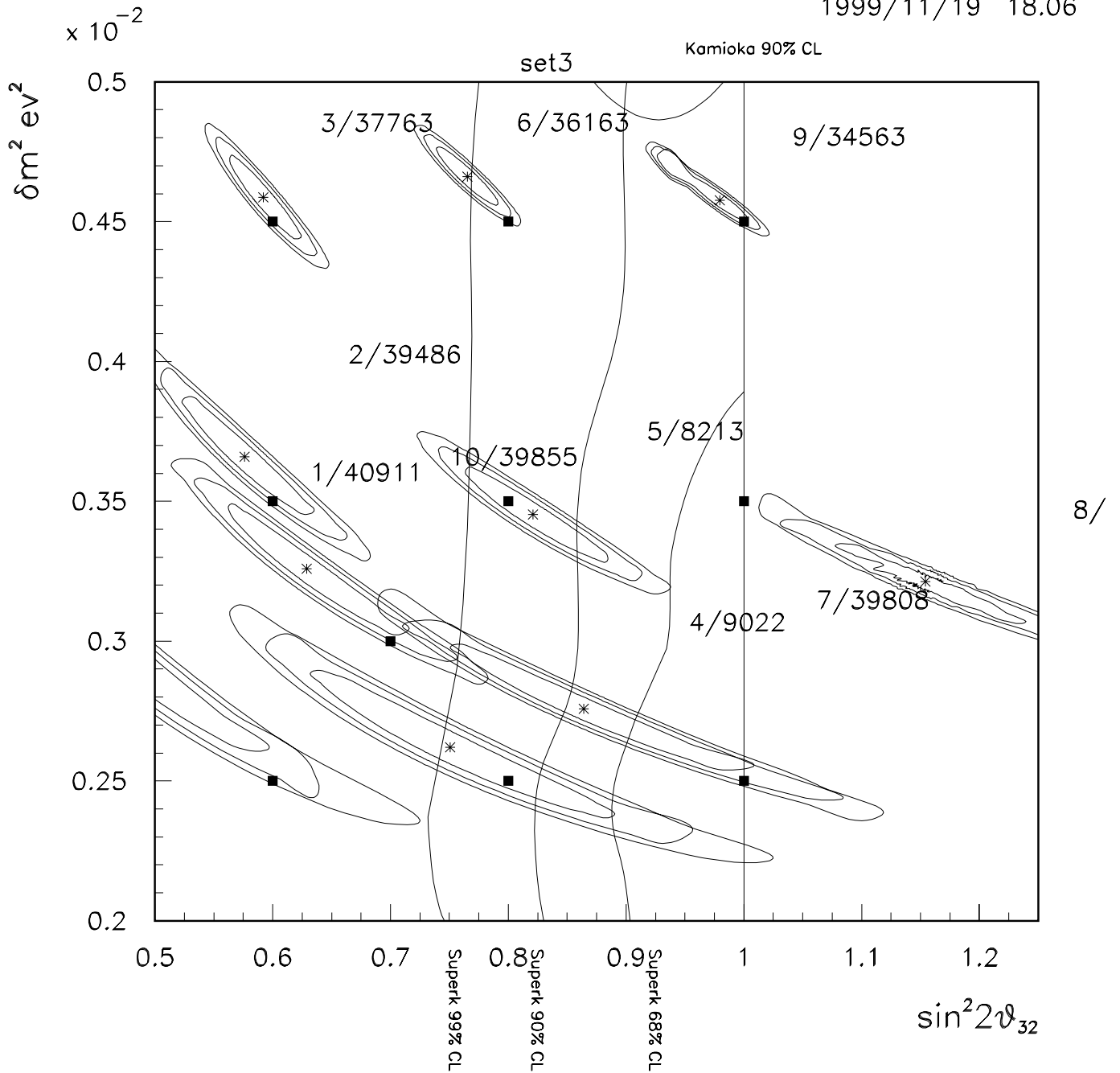


Figure 4 Set 3 Error contours for 10 experimental points, at likelihood intervals of 0.5,1.0 and 1.5 corresponding to Gaussian 1σ , 1.4σ and 1.7σ respectively. The dark rectangles denote the generated points and the *'s show the fitted points. Fitting sequence numbers and the number of events at each point are shown . SuperKamioka and Kamioka atmospheric error contours may be seen superimposed.

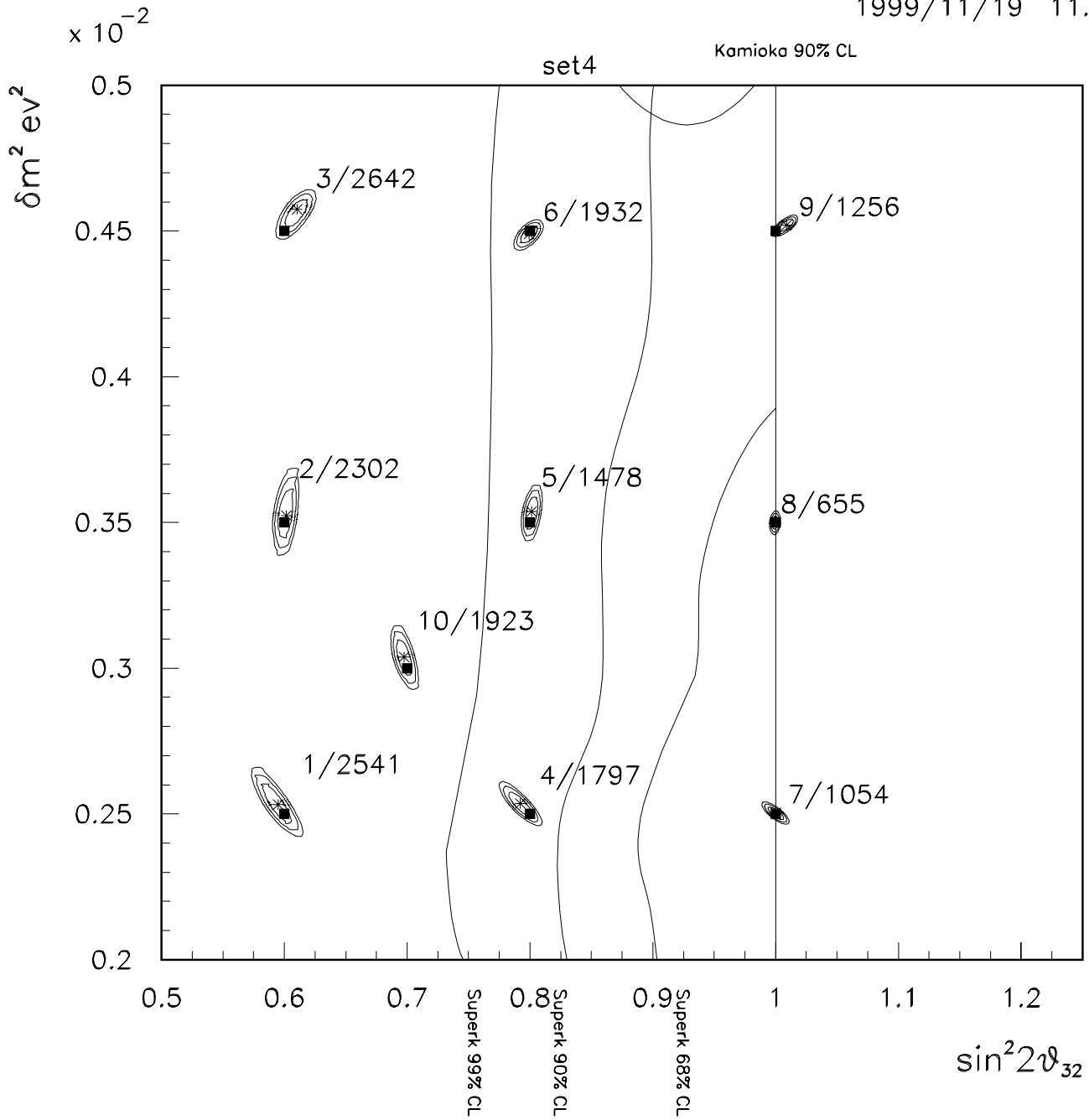


Figure 5 Set 4- Error contours for 10 experimental points, at likelihood intervals of 0.5,1.0 and 1.5 corresponding to Gaussian 1σ , 1.4σ and 1.7σ respectively. The dark rectangles denote the generated points and the *'s show the fitted points. Fitting sequence numbers and the number of events at each point are shown . SuperKamioka and Kamioka atmospheric error contours may be seen superimposed.

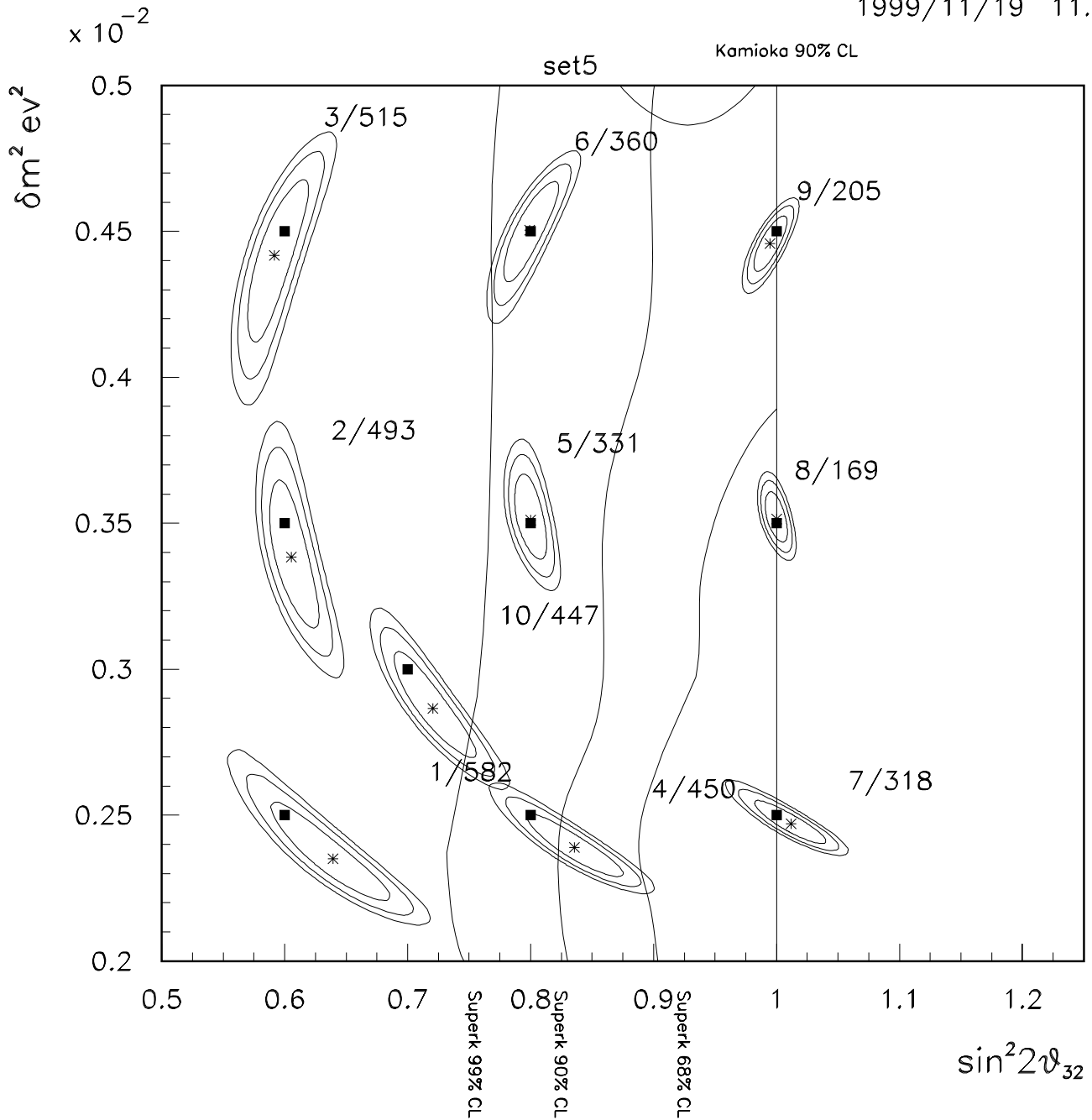


Figure 6 Set 5- Error contours for 10 experimental points, at likelihood intervals of 0.5,1.0 and 1.5 corresponding to Gaussian 1σ , 1.4σ and 1.7σ respectively. The dark rectangles denote the generated points and the *'s show the fitted points. Fitting sequence numbers and the number of events at each point are shown . SuperKamioka and Kamioka atmospheric error contours may be seen superimposed.

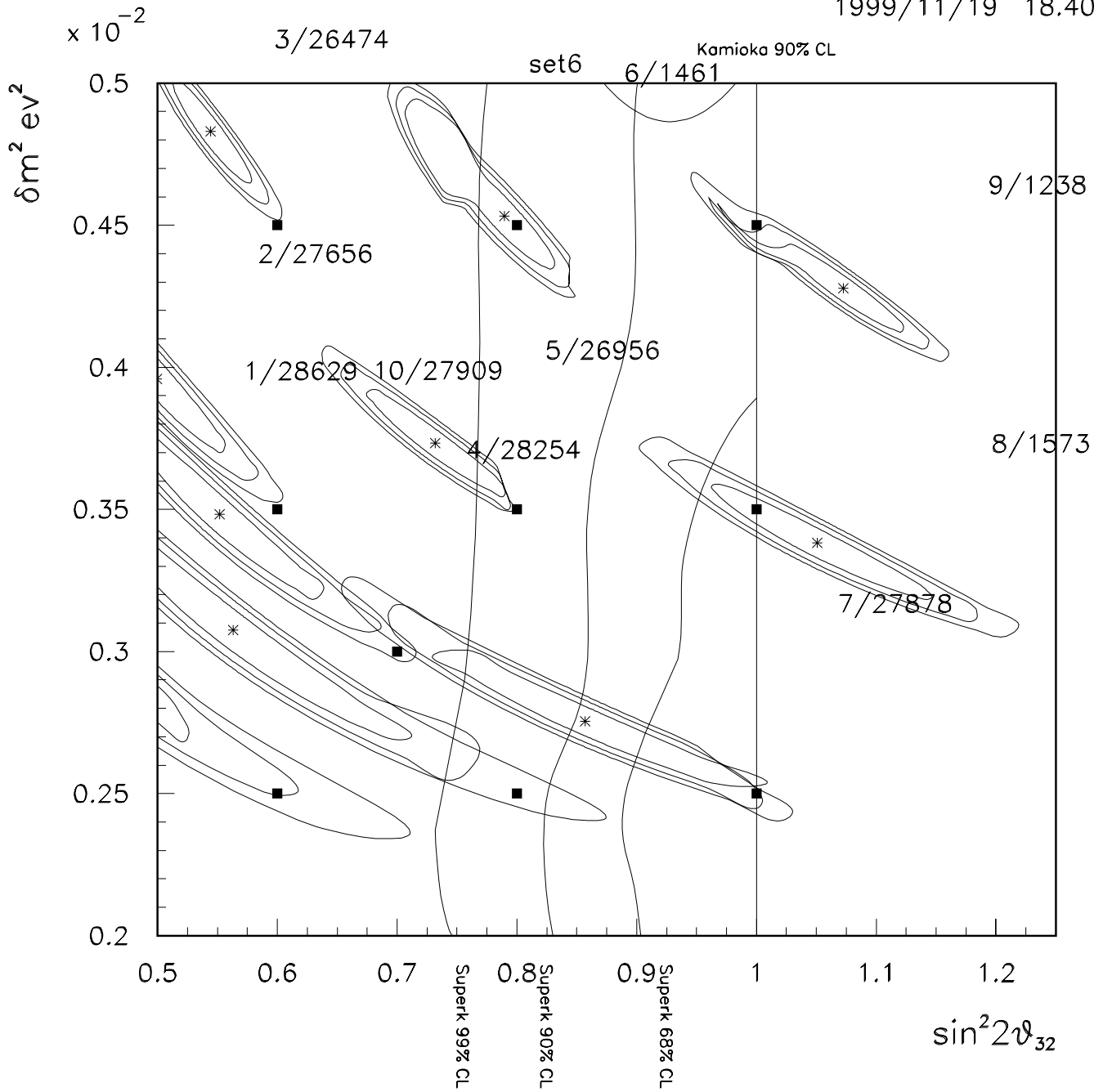


Figure 7 Set 6- Error contours for 10 experimental points, at likelihood intervals of 0.5,1.0 and 1.5 corresponding to Gaussian 1σ , 1.4σ and 1.7σ respectively. The dark rectangles denote the generated points and the *'s show the fitted points. Fitting sequence numbers and the number of events at each point are shown . SuperKamioka and Kamioka atmospheric error contours may be seen superimposed.

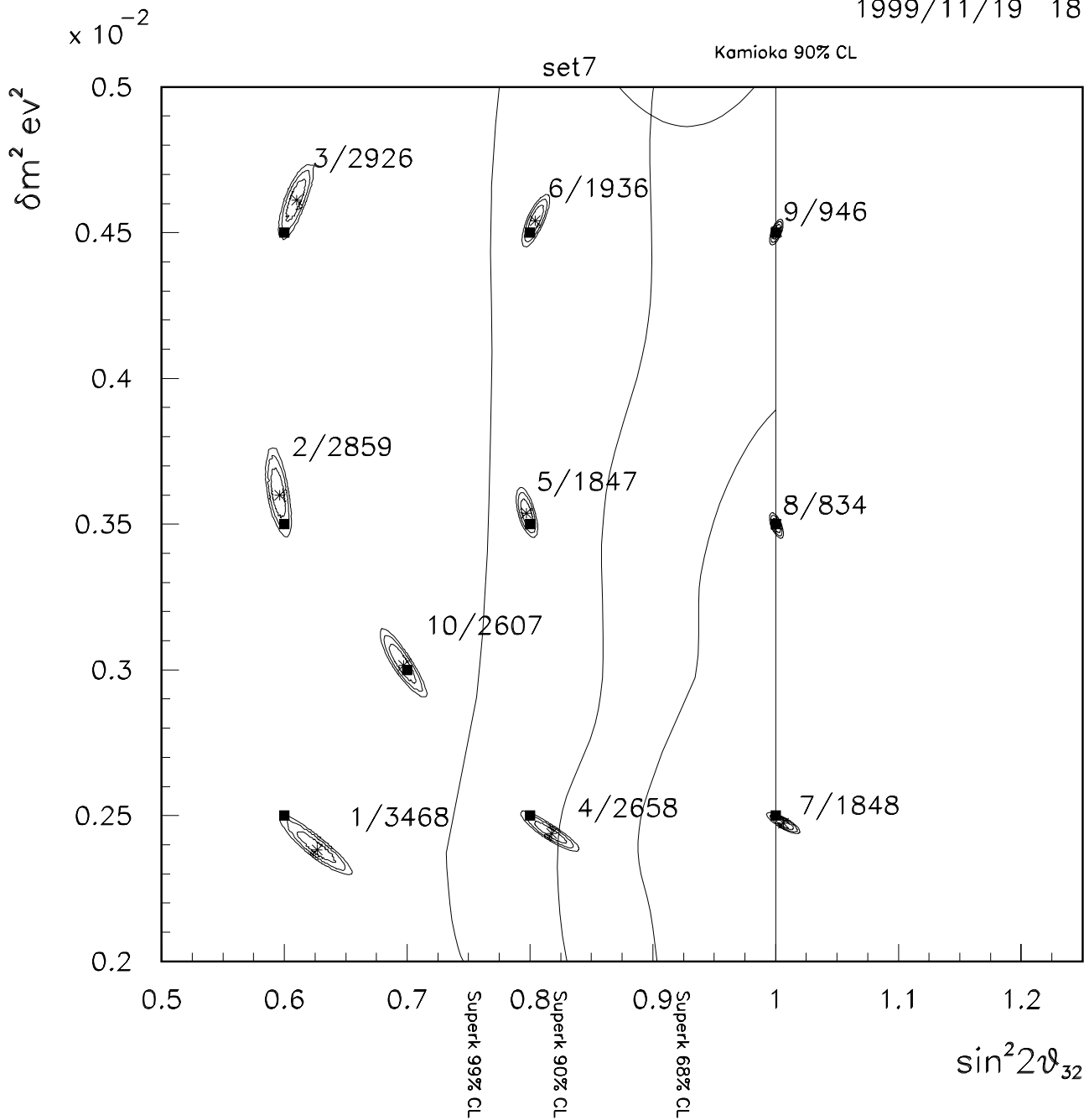


Figure 8 Set 7 Error contours for 10 experimental points, at likelihood intervals of 0.5,1.0 and 1.5 corresponding to Gaussian 1σ , 1.4σ and 1.7σ respectively. The dark rectangles denote the generated points and the *'s show the fitted points. Fitting sequence numbers and the number of events at each point are shown . SuperKamioka and Kamioka atmospheric error contours may be seen superimposed.

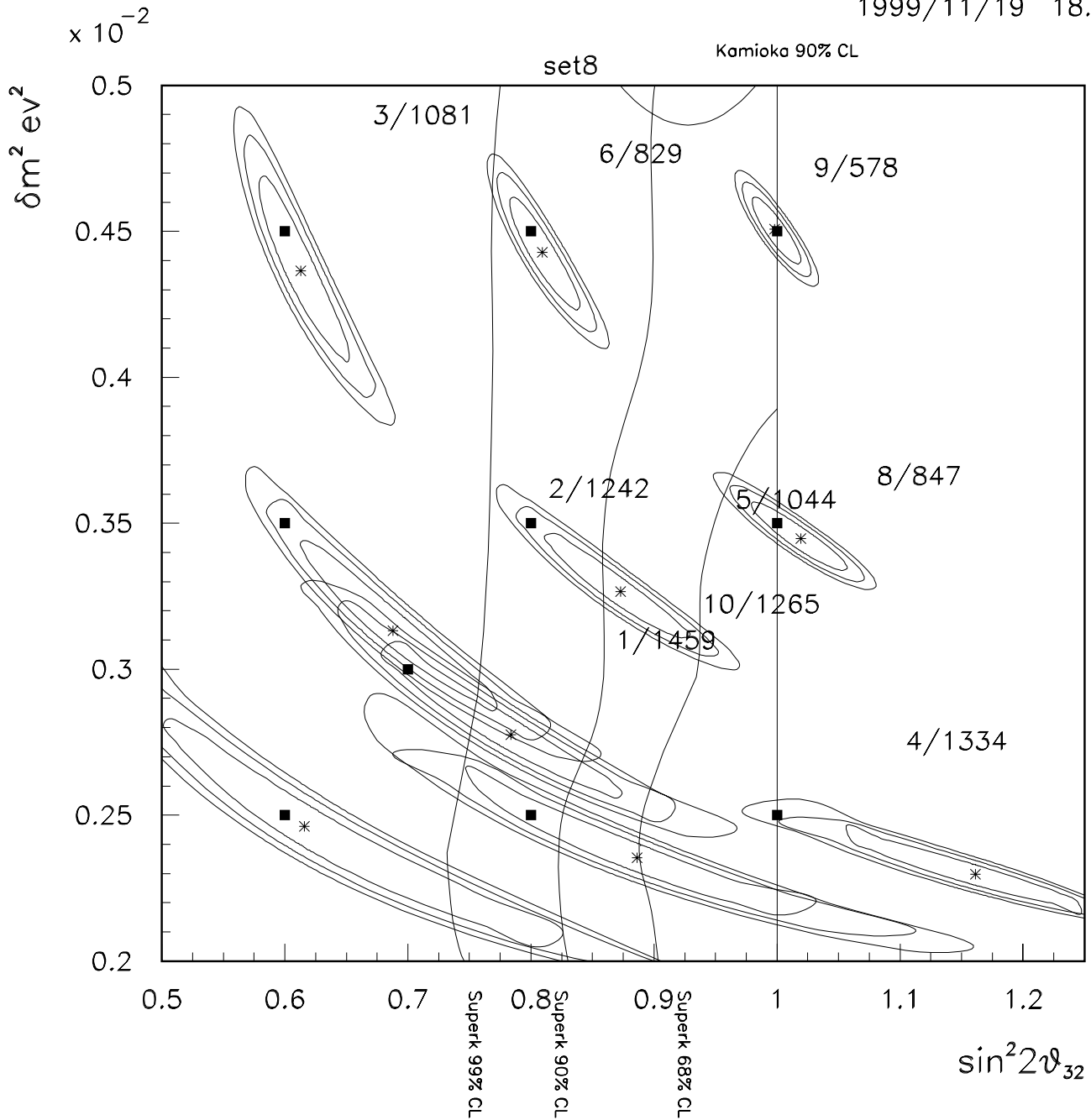


Figure9 Set 8- Error contours for 10 experimental points, at likelihood intervals of 0.5,1.0 and 1.5 corresponding to Gaussian 1σ , 1.4σ and 1.7σ respectively. The dark rectangles denote the generated points and the *'s show the fitted points. Fitting sequence numbers and the number of events at each point are shown . SuperKamioka and Kamioka atmospheric error contours may be seen superimposed.

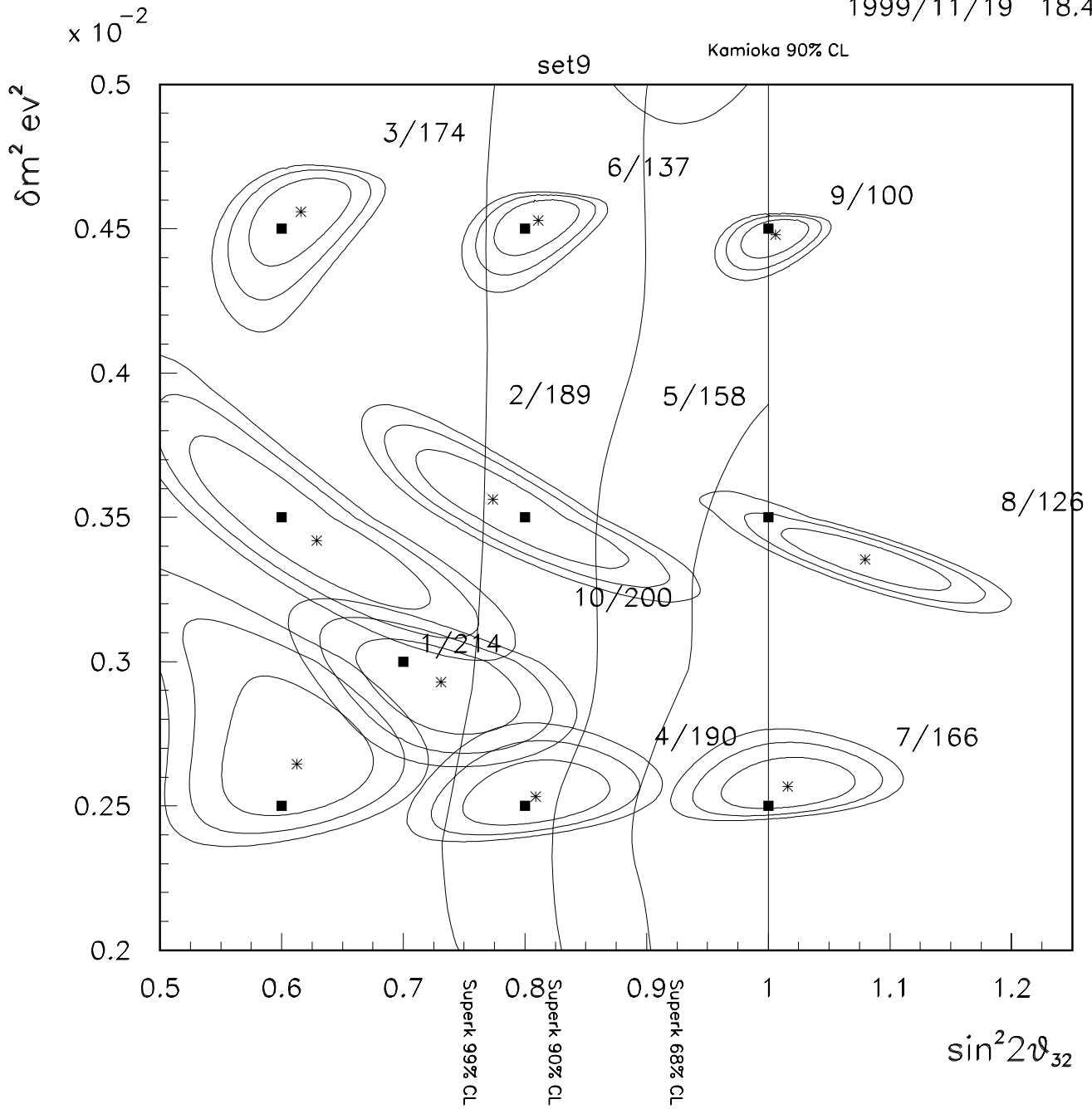


Figure 10 Set 9- Error contours for 10 experimental points, at likelihood intervals of 0.5,1.0 and 1.5 corresponding to Gaussian 1σ , 1.4σ and 1.7σ respectively. The dark rectangles denote the generated points and the *'s show the fitted points. Fitting sequence numbers and the number of events at each point are shown . SuperKamioka and Kamioka atmospheric error contours may be seen superimposed.

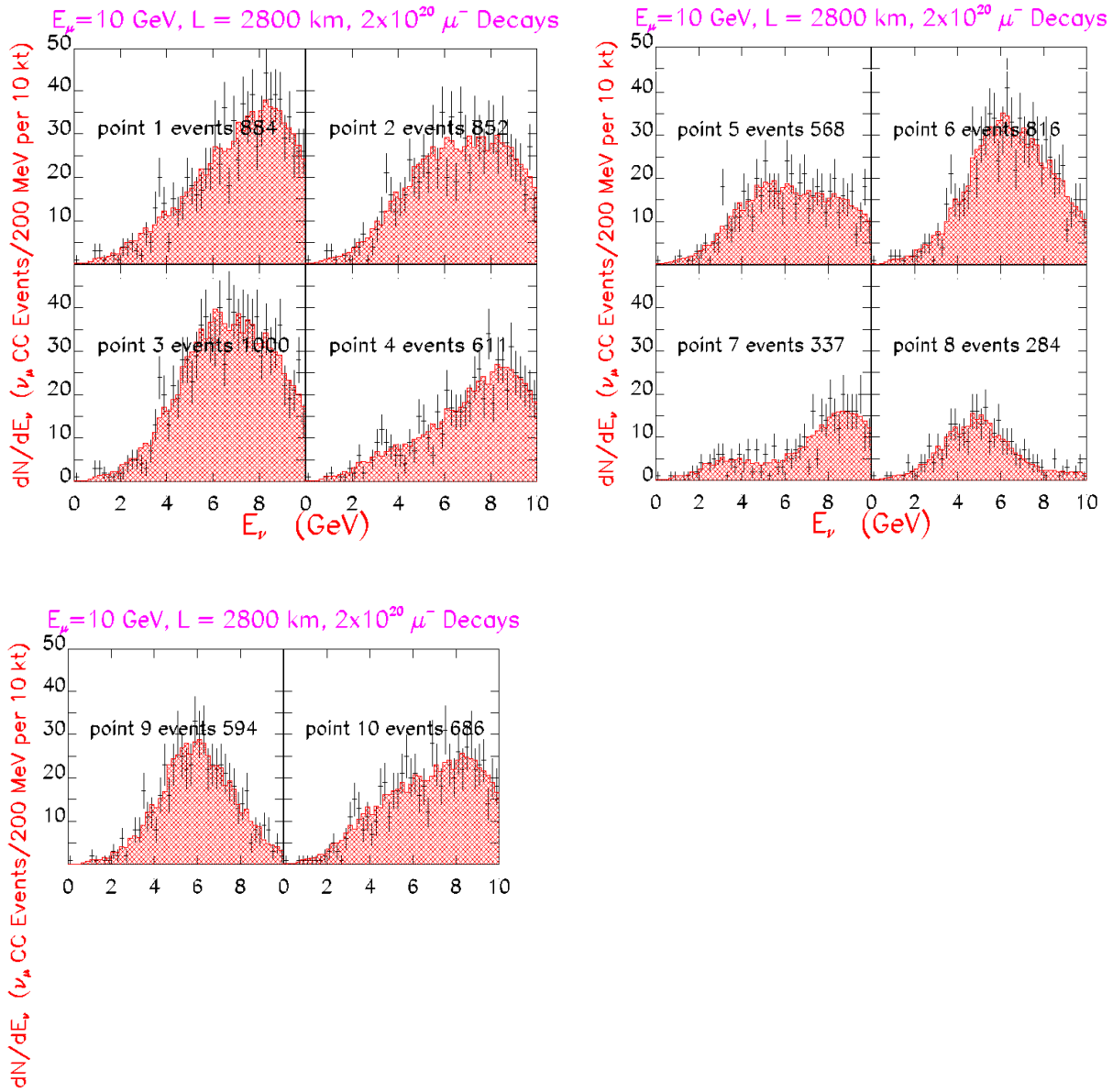


Figure 11 The experimental histograms (with error bars) vs the theoretical fits (hatched) for the 10 points in $\delta m^2, \sin^2 2\theta$ space for set 1.

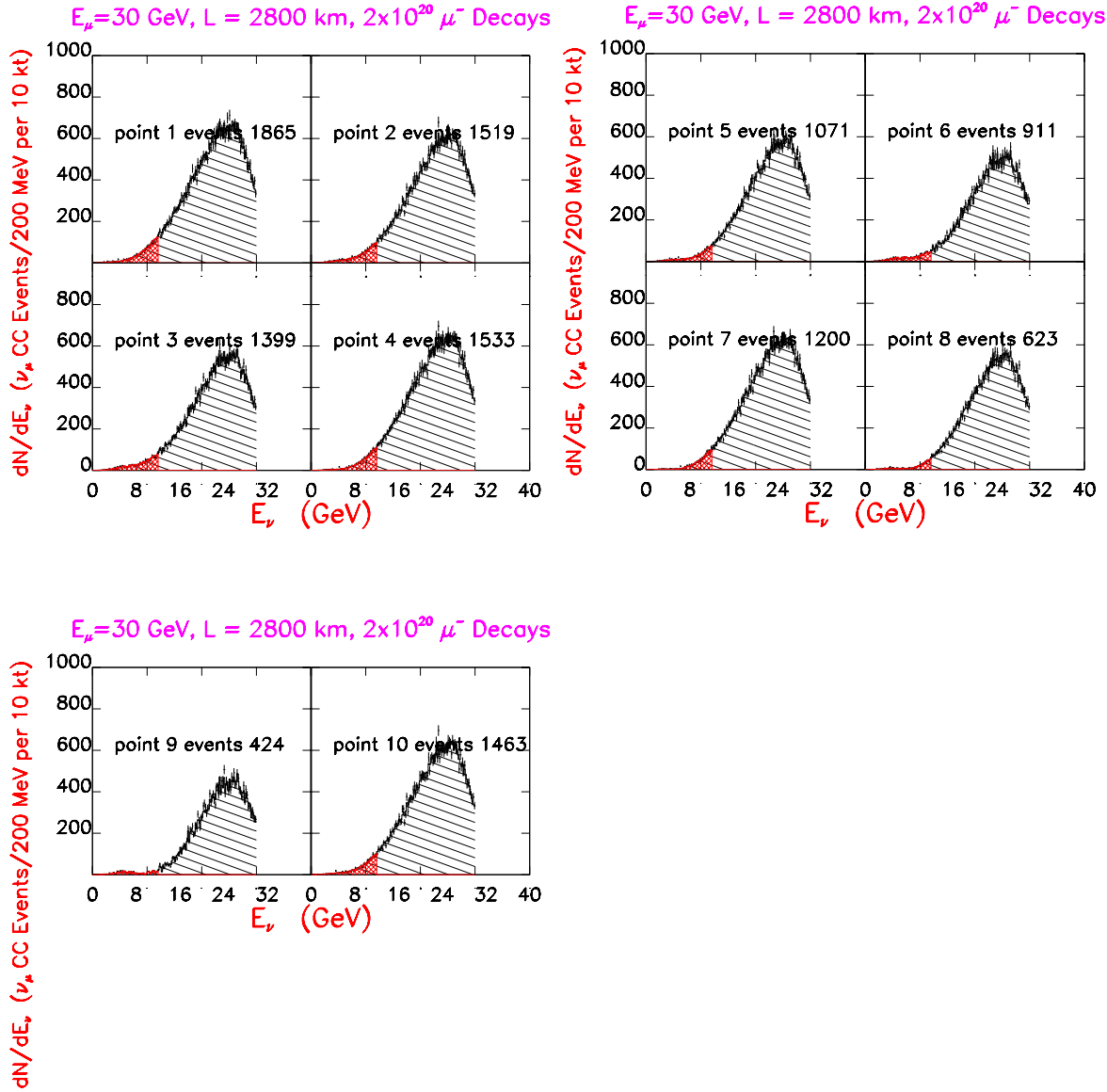


Figure 12 The experimental histograms (with error bars) vs the theoretical fits (hatched) for the 10 points in $\delta m^2, \sin^2 2\theta$ space for set 2.

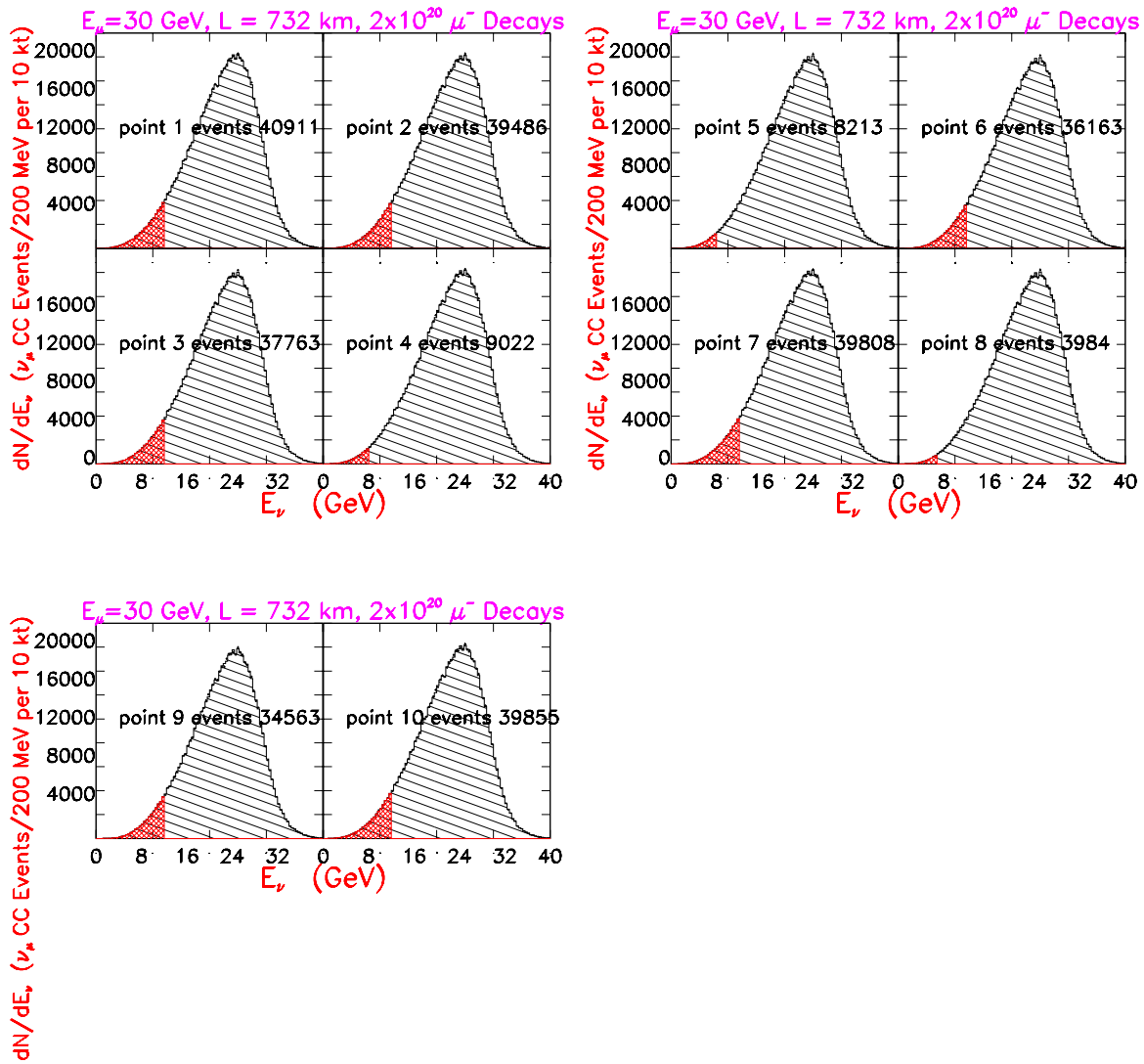


Figure 13 The experimental histograms (with error bars) vs the theoretical fits (hatched) for the 10 points in $\delta m^2, \sin^2 2\theta$ space for set 3.

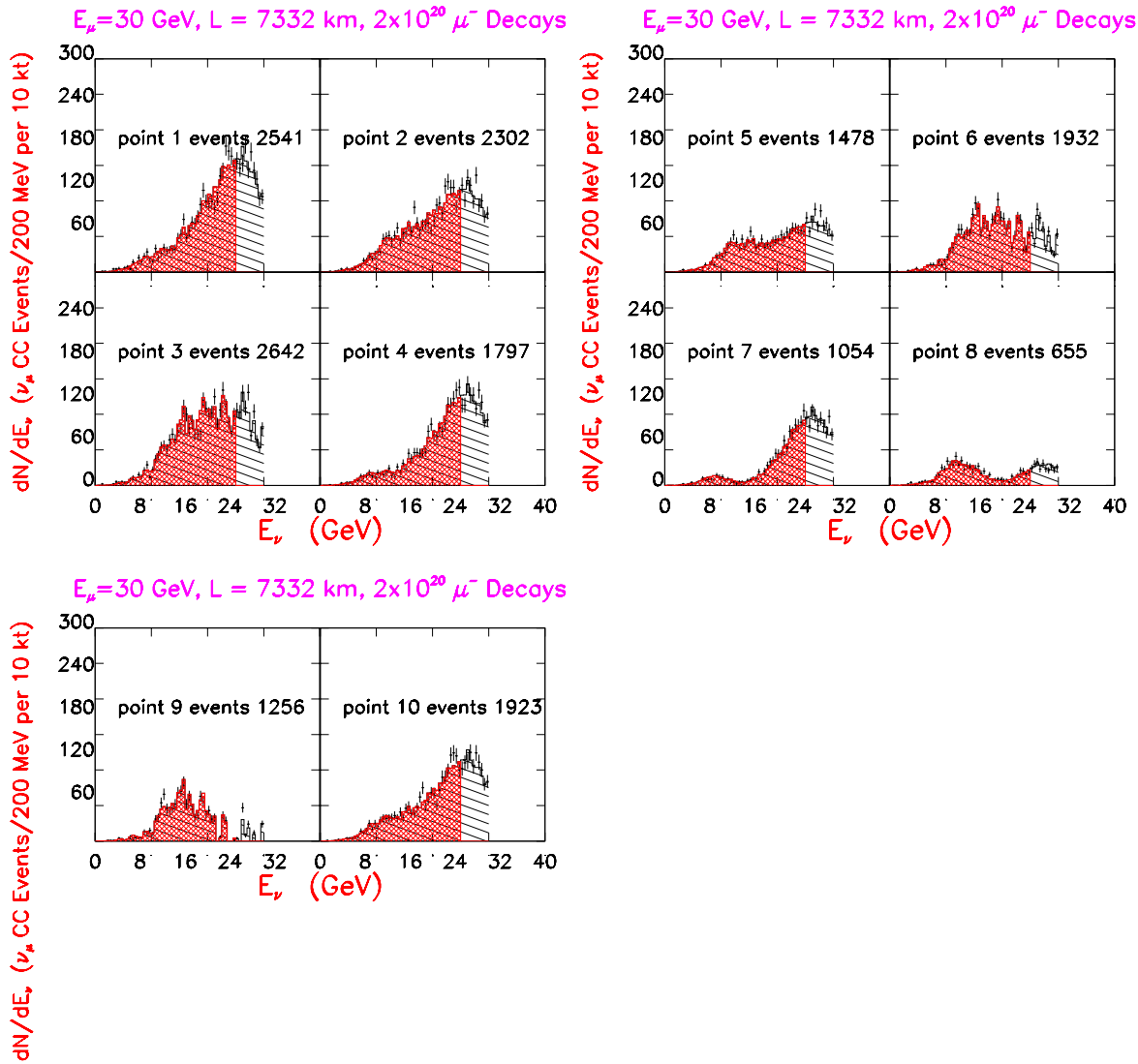


Figure 14 The experimental histograms (with error bars) vs the theoretical fits (hatched) for the 10 points in $\delta m^2, \sin^2 2\theta$ space for set 4.

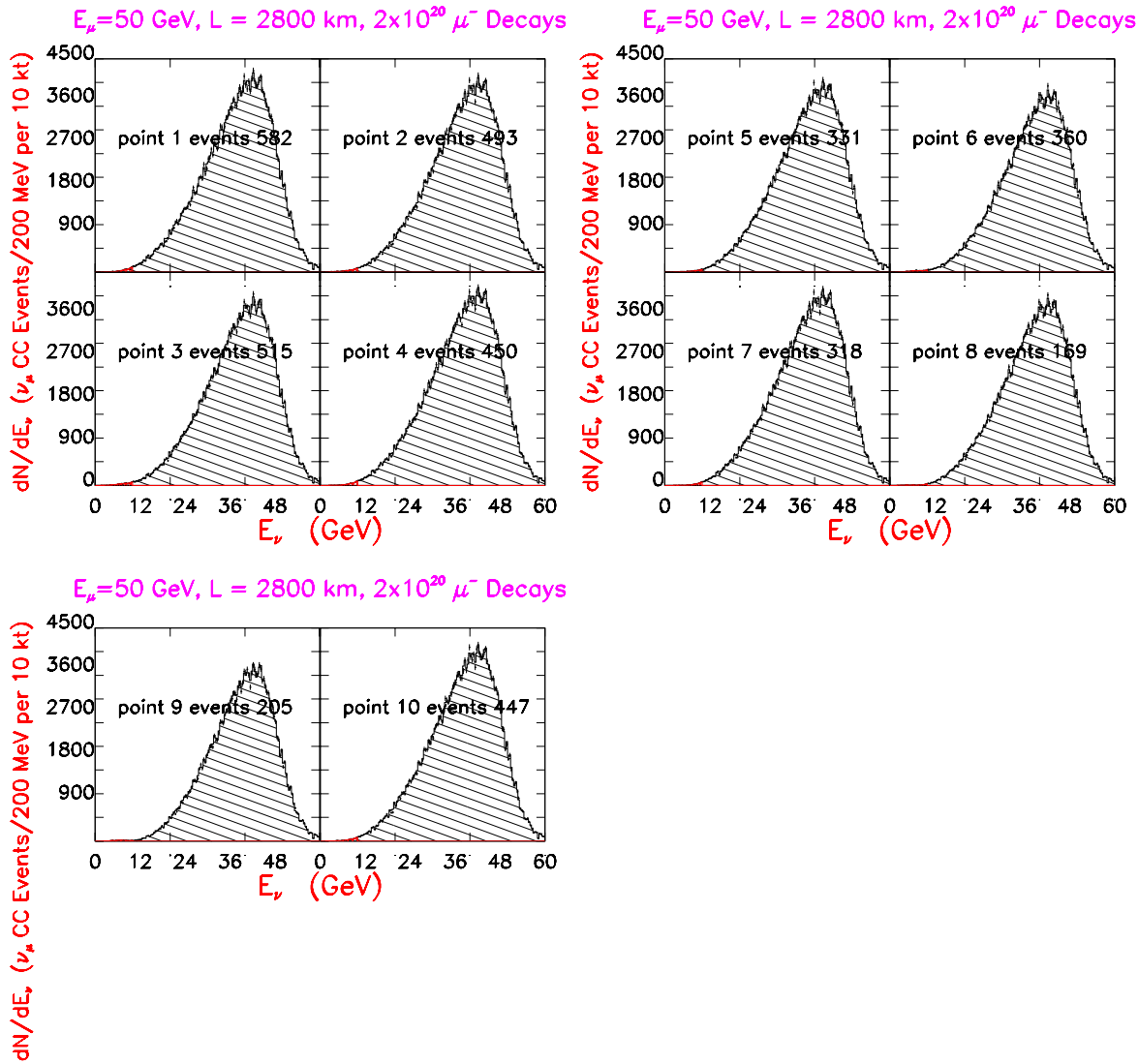


Figure 15 The experimental histograms (with error bars) vs the theoretical fits (hatched) for the 10 points in δm^2 , $\sin^2 2\theta$ space for set 5.

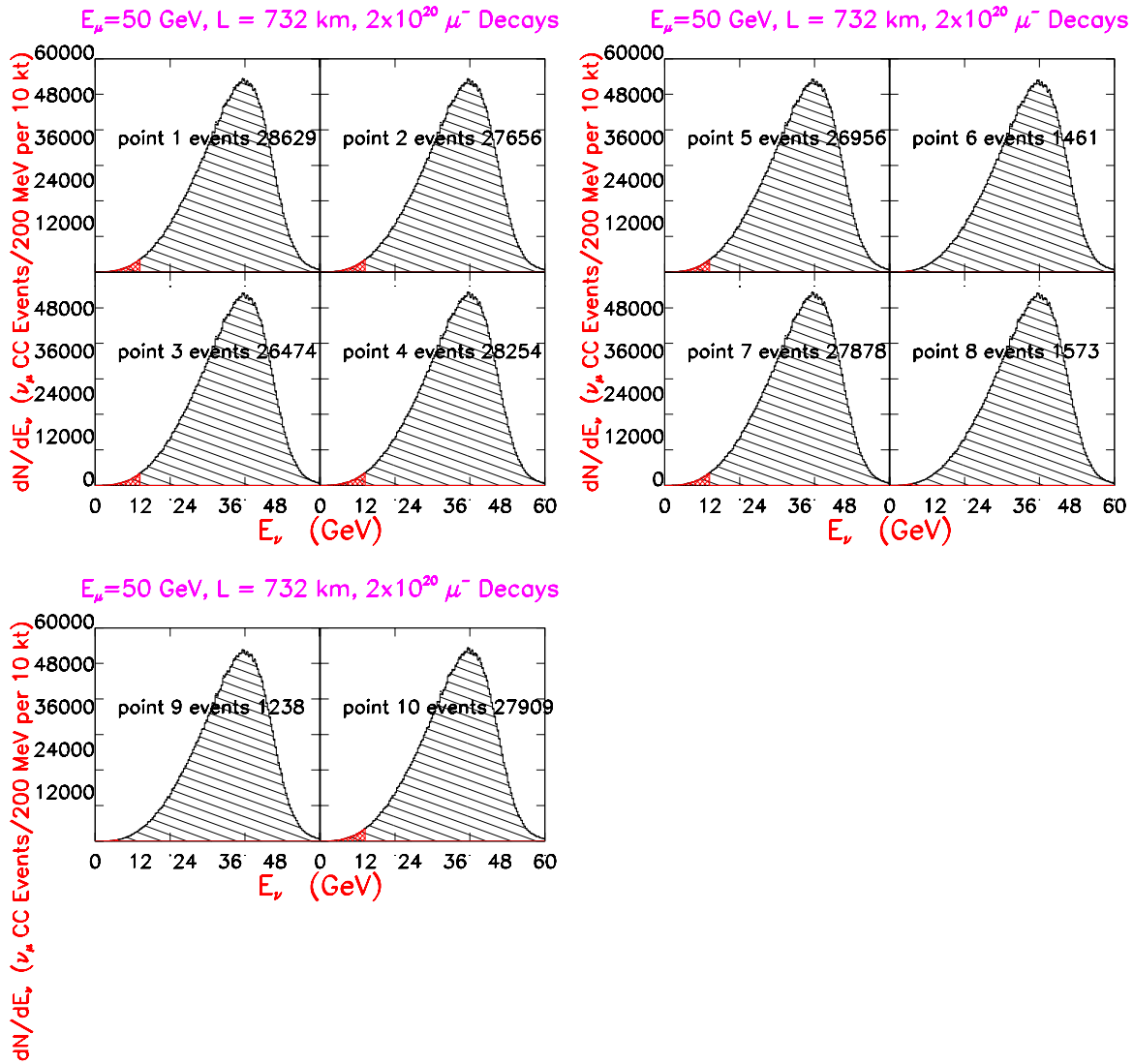


Figure 16 The experimental histograms (with error bars) vs the theoretical fits (hatched) for the 10 points in $\delta m^2, \sin^2 2\theta$ space for set 6.

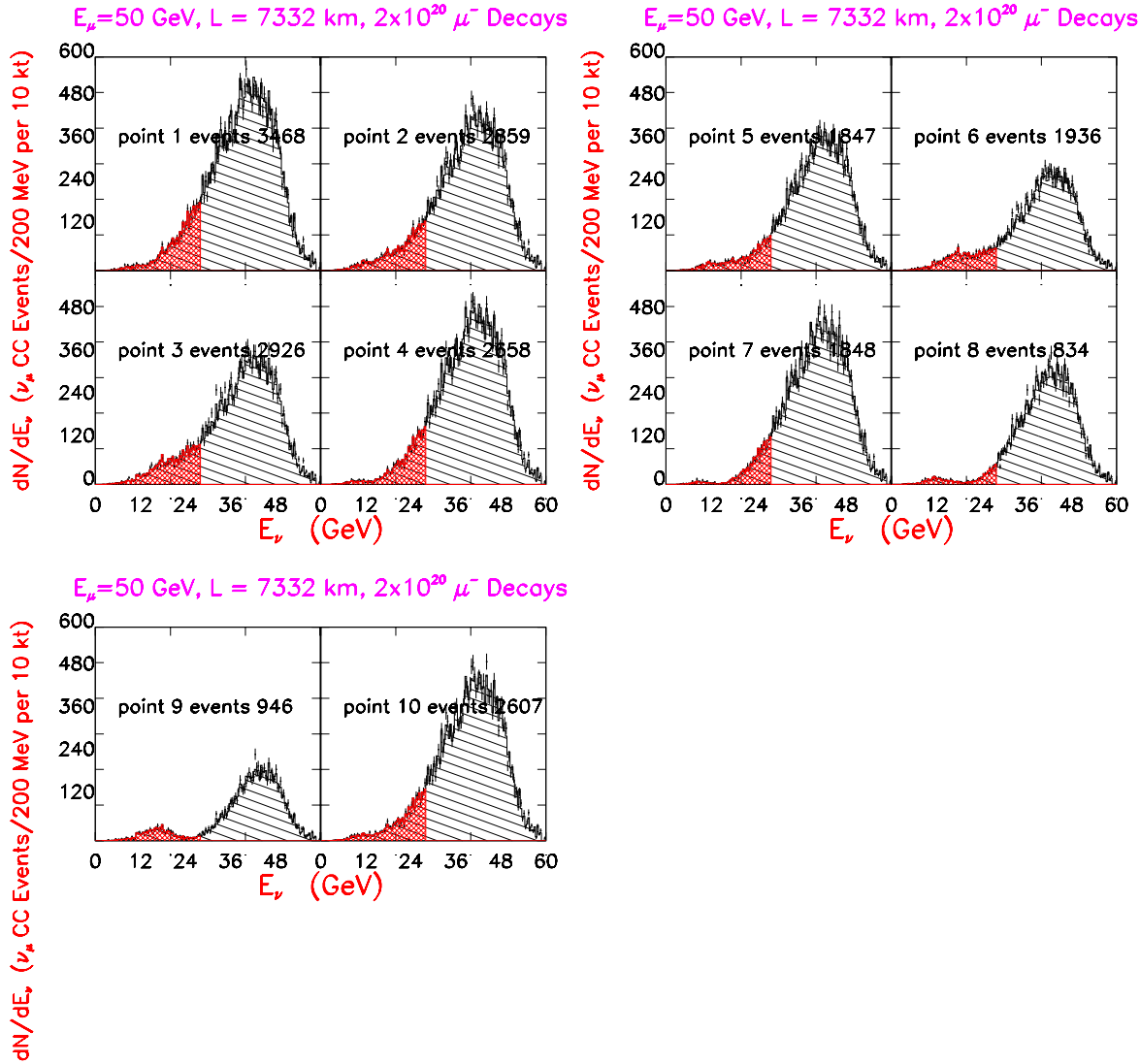


Figure 17 The experimental histograms (with error bars) vs the theoretical fits (hatched) for the 10 points in $\delta m^2, \sin^2 2\theta$ space for set 7.

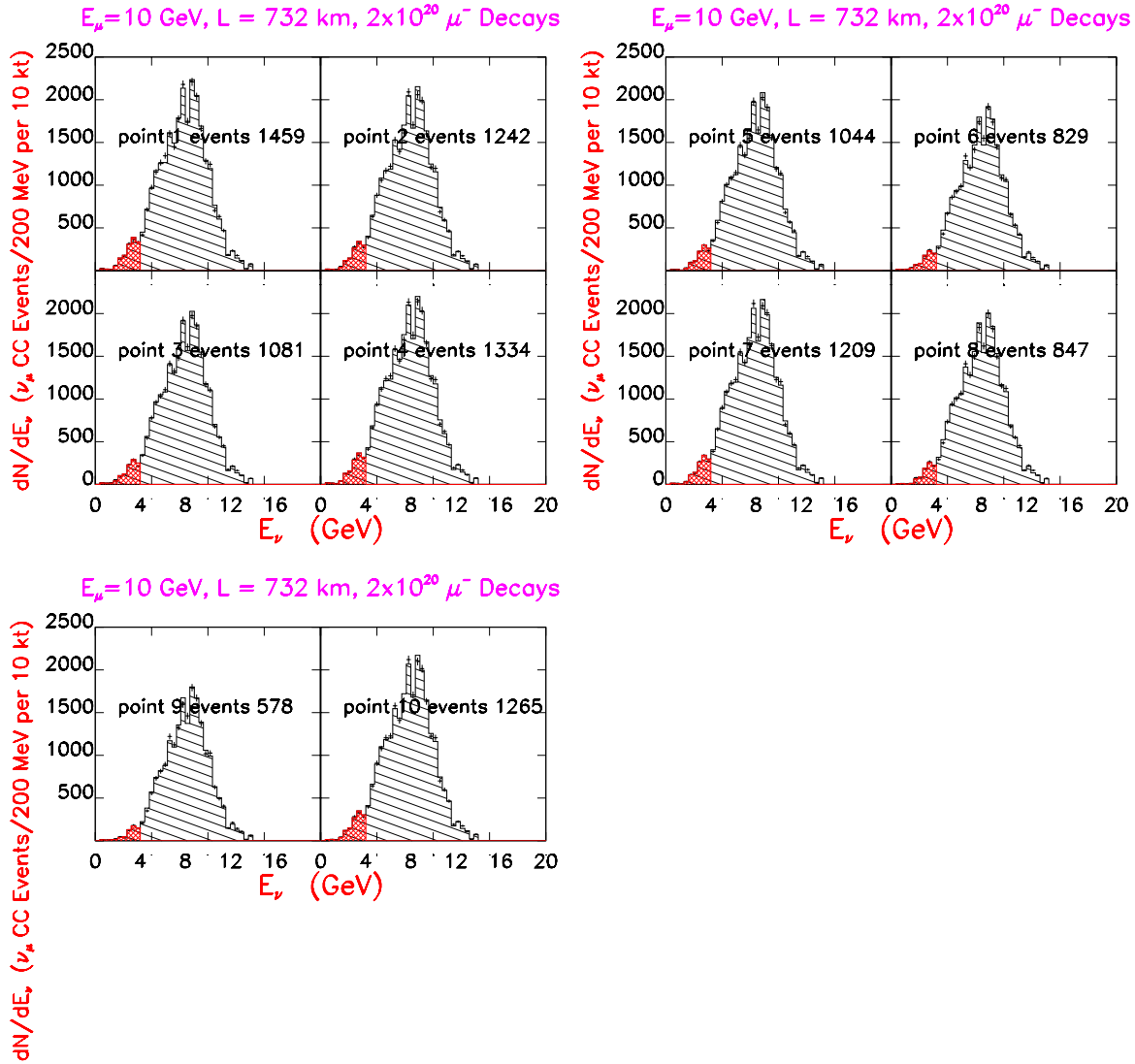


Figure 18 The experimental histograms (with error bars) vs the theoretical fits (hatched) for the 10 points in $\delta m^2, \sin^2 2\theta$ space for set 8.

Table 2 Result of fits and errors for 10 points in $\sin^2 2\theta$, δm^2 space Set 1.

Point	events	$\sin^2 2\theta_{32}$ Generated	$\sin^2 2\theta_{32}$ Fitted	$\sin^2 2\theta_{32}$ error	% \sin^2 $2\theta_{32}$ error	δm^2 generated	δm^2 fitted	δm^2 error	% δm^2 error
1	884	0.600E+00	0.601E+00	0.383E-01	6.37	0.250E-02	0.248E-02	0.242E-03	9.73
2	852	0.600E+00	0.604E+00	0.328E-01	5.44	0.350E-02	0.355E-02	0.341E-03	9.62
3	1038	0.600E+00	0.618E+00	0.105E+00	16.91	0.450E-02	0.458E-02	0.409E-03	8.94
4	611	0.800E+00	0.805E+00	0.323E-01	4.01	0.250E-02	0.247E-02	0.149E-03	6.03
5	568	0.800E+00	0.797E+00	0.217E-01	2.72	0.350E-02	0.347E-02	0.192E-03	5.55
6	816	0.800E+00	0.833E+00	0.888E-01	10.66	0.450E-02	0.460E-02	0.257E-03	5.57
7	337	0.100E+01	0.100E+01	0.224E-01	2.24	0.250E-02	0.250E-02	0.890E-04	3.56
8	284	0.100E+01	0.100E+01	0.111E-01	1.11	0.350E-02	0.353E-02	0.862E-04	2.44
9	594	0.100E+01	0.999E+00	0.657E-01	6.58	0.450E-02	0.450E-02	0.184E-03	4.07
10	686	0.700E+00	0.699E+00	0.193E-01	2.77	0.300E-02	0.300E-02	0.234E-03	7.80

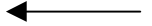


Table 3 Result of fits and errors for 10 points in $\sin^2 2\theta$, δm^2 space Set 2.

Point	events	$\sin^2 2\theta_{32}$ Generated	$\sin^2 2\theta_{32}$ Fitted	$\sin^2 2\theta_{32}$ error	% \sin^2 $2\theta_{32}$ error	δm^2 generated	δm^2 fitted	δm^2 error	% δm^2 error
1	1865	0.600E+00	0.629E+00	0.741E-01	11.78	0.250E-02	0.240E-02	0.230E-03	9.55
2	1519	0.600E+00	0.598E+00	0.289E-01	4.84	0.350E-02	0.351E-02	0.255E-03	7.27
3	1399	0.600E+00	0.601E+00	0.159E-01	2.64	0.450E-02	0.448E-02	0.223E-03	4.98
4	1533	0.800E+00	0.814E+00	0.623E-01	7.65	0.250E-02	0.246E-02	0.163E-03	6.60
5	1071	0.800E+00	0.800E+00	0.243E-01	3.03	0.350E-02	0.350E-02	0.155E-03	4.44
6	911	0.800E+00	0.798E+00	0.127E-01	1.59	0.450E-02	0.457E-02	0.144E-03	3.16
7	1200	0.100E+01	0.102E+01	0.419E-01	4.12	0.250E-02	0.248E-02	0.887E-04	3.58
8	623	0.100E+01	0.100E+01	0.202E-01	2.01	0.350E-02	0.349E-02	0.110E-03	3.15
9	424	0.100E+01	0.998E+00	0.847E-02	0.85	0.450E-02	0.453E-02	0.645E-04	1.42
10	1463	0.700E+00	0.698E+00	0.511E-01	7.33	0.300E-02	0.301E-02	0.244E-03	8.10



Table 4 Result of fits and errors for 10 points in $\sin^2 2\theta$, δm^2 space Set 3.

Point	events	$\sin^2 2\theta_{32}$ Generated	$\sin^2 2\theta_{32}$ Fitted	$\sin^2 2\theta_{32}$ error	% \sin^2 $2\theta_{32}$ error	δm^2 generated	δm^2 fitted	δm^2 error	% δm^2 error
1	40911	0.600E+00	0.467E+00	0.205E+00	43.98	0.250E-02	0.298E-02	0.744E-03	24.98
2	39486	0.600E+00	0.576E+00	0.110E+00	19.11	0.350E-02	0.366E-02	0.421E-03	11.49
3	37763	0.600E+00	0.592E+00	0.600E-01	10.14	0.450E-02	0.459E-02	0.296E-03	6.46
4	9022	0.800E+00	0.751E+00	0.253E+00	33.71	0.250E-02	0.262E-02	0.521E-03	19.89
5	8213	0.800E+00	0.821E+00	0.121E+00	14.69	0.350E-02	0.345E-02	0.335E-03	9.70
6	36163	0.800E+00	0.765E+00	0.517E-01	6.75	0.450E-02	0.466E-02	0.205E-03	4.41
7	39808	0.100E+01	0.864E+00	0.246E+00	28.52	0.250E-02	0.276E-02	0.448E-03	16.25
8	3984	0.100E+01	0.115E+01	0.156E+00	13.53	0.350E-02	0.321E-02	0.284E-03	8.86
9	34563	0.100E+01	0.980E+00	0.768E-01	7.84	0.450E-02	0.458E-02	0.246E-03	5.38
10	39855	0.700E+00	0.629E+00	0.151E+00	23.95	0.300E-02	0.326E-02	0.463E-03	14.20

Table 5 Result of fits and errors for 10 points in $\sin^2 2\theta$, δm^2 space Set 4.

Point	events	$\text{Sin}^2 2\theta_{32}$ Generat ed	$\text{Sin}^2 2\theta_{32}$ Fitted	$\text{Sin}^2 2\theta_{32}$ error	% Sin^2 $2\theta_{32}$ error	δm^2 generat ed	δm^2 fitted	δm^2 error	% δm^2 error
1	2541	0.600E+00	0.595E+00	0.227E-01	3.82	0.250E-02	0.253E-02	0.135E-03	5.31
2	2302	0.600E+00	0.602E+00	0.123E-01	2.04	0.350E-02	0.352E-02	0.165E-03	4.67
3	2642	0.600E+00	0.610E+00	0.184E-01	3.01	0.450E-02	0.458E-02	0.947E-04	2.07
4	1797	0.800E+00	0.792E+00	0.194E-01	2.45	0.250E-02	0.254E-02	0.843E-04	3.33
5	1478	0.800E+00	0.801E+00	0.985E-02	1.23	0.350E-02	0.354E-02	0.109E-03	3.08
6	1932	0.800E+00	0.799E+00	0.137E-01	1.71	0.450E-02	0.449E-02	0.578E-04	1.29
7	1054	0.100E+01	0.100E+01	0.126E-01	1.26	0.250E-02	0.250E-02	0.431E-04	1.72
8	655	0.100E+01	0.100E+01	0.568E-02	0.57	0.350E-02	0.350E-02	0.427E-04	1.22
9	1256	0.100E+01	0.101E+01	0.123E-01	1.22	0.450E-02	0.452E-02	0.420E-04	0.93
10	1923	0.700E+00	0.697E+00	0.124E-01	1.78	0.300E-02	0.304E-02	0.120E-03	3.94

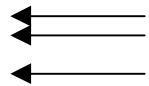


Table 6 Result of fits and errors for 10 points in $\sin^2 2\theta$, δm^2 space Set 5.

Point	events	$\text{Sin}^2 2\theta_{32}$ Generat ed	$\text{Sin}^2 2\theta_{32}$ Fitted	$\text{Sin}^2 2\theta_{32}$ error	% Sin^2 $2\theta_{32}$ error	δm^2 generat ed	δm^2 fitted	δm^2 error	% δm^2 error
1	582	0.600E+00	0.639E+00	0.964E-01	15.08	0.250E-02	0.235E-02	0.335E-03	14.26
2	493	0.600E+00	0.606E+00	0.401E-01	6.62	0.350E-02	0.338E-02	0.506E-03	14.96
3	515	0.600E+00	0.592E+00	0.494E-01	8.35	0.450E-02	0.442E-02	0.556E-03	12.59
4	450	0.800E+00	0.836E+00	0.780E-01	9.33	0.250E-02	0.239E-02	0.215E-03	8.99
5	331	0.800E+00	0.800E+00	0.259E-01	3.24	0.350E-02	0.351E-02	0.291E-03	8.30
6	360	0.800E+00	0.799E+00	0.446E-01	5.58	0.450E-02	0.450E-02	0.343E-03	7.62
7	318	0.100E+01	0.101E+01	0.577E-01	5.70	0.250E-02	0.247E-02	0.146E-03	5.92
8	169	0.100E+01	0.100E+01	0.180E-01	1.80	0.350E-02	0.352E-02	0.172E-03	4.89
9	205	0.100E+01	0.995E+00	0.270E-01	2.71	0.450E-02	0.446E-02	0.189E-03	4.24
10	447	0.700E+00	0.720E+00	0.664E-01	9.21	0.300E-02	0.287E-02	0.363E-03	12.66

Table 7 Result of fits and errors for 10 points in $\sin^2 2\theta$, δm^2 space Set 6.

Point	events	$\text{Sin}^2 2\theta_{32}$ Generat ed	$\text{Sin}^2 2\theta_{32}$ Fitted	$\text{Sin}^2 2\theta_{32}$ error	% Sin^2 $2\theta_{32}$ erro r	δm^2 generat ed	δm^2 fitted	δm^2 error	% δm^2 error
1	28629	0.600E+00	0.402E+00	0.212E+00	52.86	0.250E-02	0.319E-02	0.958E-03	30.03
2	27656	0.600E+00	0.500E+00	0.105E+00	21.06	0.350E-02	0.396E-02	0.514E-03	12.99
3	26474	0.600E+00	0.544E+00	0.657E-01	12.07	0.450E-02	0.483E-02	0.367E-03	7.59
4	28254	0.800E+00	0.563E+00	0.242E+00	43.04	0.250E-02	0.308E-02	0.757E-03	24.61
5	26956	0.800E+00	0.732E+00	0.115E+00	15.65	0.350E-02	0.373E-02	0.373E-03	9.98
6	1461	0.800E+00	0.789E+00	0.124E+00	15.77	0.450E-02	0.453E-02	0.592E-03	13.05
7	27878	0.100E+01	0.857E+00	0.263E+00	30.70	0.250E-02	0.276E-02	0.479E-03	17.40
8	1573	0.100E+01	0.105E+01	0.182E+00	17.28	0.350E-02	0.338E-02	0.400E-03	11.82
9	1238	0.100E+01	0.107E+01	0.151E+00	14.07	0.450E-02	0.428E-02	0.418E-03	9.77
10	27909	0.700E+00	0.552E+00	0.159E+00	28.79	0.300E-02	0.348E-02	0.597E-03	17.14

Table 8 Result of fits and errors for 10 points in $\sin^2 2\theta$, δm^2 space Set 7.

Point	events	$\sin^2 2\theta_{32}$ Generated	$\sin^2 2\theta_{32}$ Fitted	$\sin^2 2\theta_{32}$ error	% \sin^2 $2\theta_{32}$ error	δm^2 generated	δm^2 fitted	δm^2 error	% δm^2 error
1	3468	0.600E+00	0.627E+00	0.313E-01	4.99	0.250E-02	0.238E-02	0.105E-03	4.40
2	2859	0.600E+00	0.596E+00	0.120E-01	2.02	0.350E-02	0.360E-02	0.171E-03	4.74
3	2926	0.600E+00	0.610E+00	0.159E-01	2.61	0.450E-02	0.461E-02	0.144E-03	3.12
4	2658	0.800E+00	0.818E+00	0.257E-01	3.14	0.250E-02	0.244E-02	0.739E-04	3.03
5	1847	0.800E+00	0.797E+00	0.100E-01	1.25	0.350E-02	0.354E-02	0.983E-04	2.78
6	1936	0.800E+00	0.804E+00	0.125E-01	1.55	0.450E-02	0.454E-02	0.103E-03	2.27
7	1848	0.100E+01	0.101E+01	0.152E-01	1.51	0.250E-02	0.247E-02	0.403E-04	1.63
8	834	0.100E+01	0.100E+01	0.640E-02	0.64	0.350E-02	0.350E-02	0.483E-04	1.38
9	946	0.100E+01	0.100E+01	0.638E-02	0.64	0.450E-02	0.450E-02	0.503E-04	1.12
10	2607	0.700E+00	0.697E+00	0.216E-01	3.09	0.300E-02	0.302E-02	0.133E-03	4.40

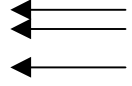


Table 9 Result of fits and errors for 10 points in $\sin^2 2\theta$, δm^2 space Set 8.

Point	events	$\sin^2 2\theta_{32}$ Generated	$\sin^2 2\theta_{32}$ Fitted	$\sin^2 2\theta_{32}$ error	% \sin^2 $2\theta_{32}$ error	δm^2 generated	δm^2 fitted	δm^2 error	% δm^2 error
1	1459	0.600E+00	0.616E+00	0.316E+00	51.28	0.250E-02	0.246E-02	0.760E-03	30.88
2	1242	0.600E+00	0.688E+00	0.158E+00	22.95	0.350E-02	0.313E-02	0.572E-03	18.26
3	1081	0.600E+00	0.613E+00	0.726E-01	11.84	0.450E-02	0.436E-02	0.630E-03	14.43
4	1334	0.800E+00	0.886E+00	0.273E+00	30.77	0.250E-02	0.235E-02	0.463E-03	19.68
5	1044	0.800E+00	0.873E+00	0.116E+00	13.34	0.350E-02	0.327E-02	0.357E-03	10.94
6	829	0.800E+00	0.809E+00	0.567E-01	7.01	0.450E-02	0.443E-02	0.385E-03	8.70
7	1209	0.100E+01	0.116E+01	0.188E+00	16.21	0.250E-02	0.230E-02	0.242E-03	10.51
8	847	0.100E+01	0.102E+01	0.770E-01	7.56	0.350E-02	0.345E-02	0.232E-03	6.74
9	578	0.100E+01	0.998E+00	0.394E-01	3.95	0.450E-02	0.451E-02	0.229E-03	5.07
10	1265	0.700E+00	0.784E+00	0.194E+00	24.76	0.300E-02	0.278E-02	0.522E-03	18.81

Table 10 Result of fits and errors for 10 points in $\sin^2 2\theta$, δm^2 space Set 9.

Point	events	$\sin^2 2\theta_{32}$ Generated	$\sin^2 2\theta_{32}$ Fitted	$\sin^2 2\theta_{32}$ error	% \sin^2 $2\theta_{32}$ error	δm^2 generated	δm^2 fitted	δm^2 error	% δm^2 error
1	214	0.600E+00	0.612E+00	0.125E+00	20.34	0.250E-02	0.265E-02	0.484E-03	18.29
2	189	0.600E+00	0.629E+00	0.197E+00	31.28	0.350E-02	0.342E-02	0.597E-03	17.45
3	174	0.600E+00	0.616E+00	0.836E-01	13.57	0.450E-02	0.456E-02	0.305E-03	6.68
4	190	0.800E+00	0.809E+00	0.121E+00	14.92	0.250E-02	0.253E-02	0.225E-03	8.90
5	158	0.800E+00	0.774E+00	0.174E+00	22.44	0.350E-02	0.356E-02	0.410E-03	11.52
6	137	0.800E+00	0.811E+00	0.699E-01	8.62	0.450E-02	0.453E-02	0.194E-03	4.28
7	166	0.100E+01	0.102E+01	0.110E+00	10.83	0.250E-02	0.257E-02	0.177E-03	6.89
8	126	0.100E+01	0.108E+01	0.139E+00	12.88	0.350E-02	0.335E-02	0.212E-03	6.32
9	100	0.100E+01	0.101E+01	0.556E-01	5.52	0.450E-02	0.448E-02	0.133E-03	2.97
10	200	0.700E+00	0.731E+00	0.135E+00	18.45	0.300E-02	0.293E-02	0.330E-03	11.25

Table 11 Summary of errors for $\sin^2 2\theta=1.0$, $\delta m^2=0.35 \times 10^{-2} \text{ eV}^2/c^4$.

Baseline length km	Muon energy GeV	Error $\sin^2 2\theta$	Error δm^2
732	10	7.6%	6.7%
732	30	14%	8.9%
732	50	17%	12%
2800	10	1.1%	2.4%
2800	30	2.0%	3.2%
2800	50	1.8%	4.9%
7332	10	13%	6.3%
7332	30	0.57%	1.2%
7332	50	0.64%	1.4%

Sensitivity with respect to δm^2 and $\sin^2 2\theta$

It is interesting to ask at what point in energy one has the maximum sensitivity to variations in $\sin^2 2\theta$ and δm^2 . Let us again neglect effects due to smearing. Then the observed energy spectrum is given by

$$\frac{dN}{dE} = \frac{dN_{no}}{dE} (1 - \cos^4 \theta_{31} \sin^2 2\theta_{32} \sin^2 (1.267 \delta m_{32}^2 L / E))$$

where dN_{no}/dE is the energy spectrum observed in the detector in the absence of oscillations. Denoting $\sin^2 2\theta_{32}$ by x , δm^2 by y , $1.267L/E$ by λ and setting $\cos^4 \theta_{31}=1$ for simplicity, and differentiating with respect to y , yields

$$\frac{\partial}{\partial y} \left(\frac{dN}{dE} \right) = \frac{dN_{no}}{dE} (-\lambda x \sin(2\lambda y))$$

This gives the rate of change of the observed energy spectrum wrt $y=\delta m^2$. In order to ask where the spectrum has an optimum, we need to differentiate the above equation wrt E (or λ) and set the derivative to zero. This yields, $\tan(2\lambda y) = -2\lambda y$, which is the condition for maximum sensitivity to δm^2 . For a given δm^2 , this

equation gives the $\lambda=1.267L/E$, that is most sensitive to δm^2 . Figure 20(a) shows the survival probability for a detector 2800 km away as a function of neutrino energy. For δm^2 of $.35 \times 10^{-2} \text{ eV}^2/\text{c}^4$, the highest energy minimum of oscillation occurs at a neutrino energy of $\sim 7.9 \text{ GeV}$. There is a secondary minimum at 1/3 this energy at 2.63 GeV. Figure 20(b) shows the derivative of this curve with respect to δm^2 . This shows a maximum sensitivity point at just above 12 GeV and another maximum sensitivity point at just below 5 GeV. Figure 20(c) shows the two functions $\cos(2\lambda y)$ and $2\lambda y \sin(2\lambda y)$. Where they intersect are the positions of maximum δm^2 sensitivity. The first solution to this happens for $2\lambda y = 2.02875$, corresponding to an energy of 12.24 GeV for $L=2800\text{km}$ and $y=.35 \times 10^{-2} \text{ eV}^2/\text{c}^4$. As regards sensitivity to $\sin^2 2\theta$, the maximum sensitivity occurs when $\sin(2\lambda y)=0$. This is automatically satisfied by the resonance condition $\sin(\lambda y)=1$. So the neutrino spectrum should be such that it should be strong where $\lambda y=1.01436$ and $\lambda y = \pi/2=1.5708$.

1999/11/20 19.13

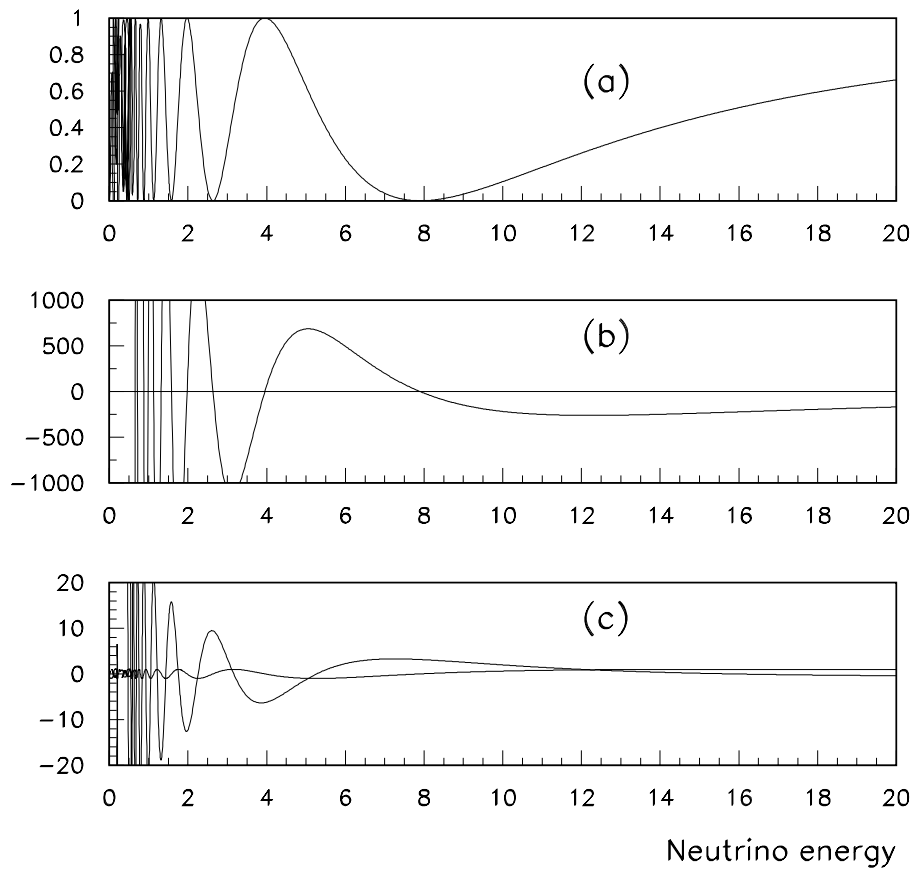


Figure 20 (a) shows the survival probability as function of neutrino energy for $\delta m^2=.35 \times 10^{-2} \text{ eV}^2/\text{c}^4$ and a 2800km baseline. (b) shows the rate of change of the survival probability with respect to δm^2 . (c) shows the two curves $\sin(2\lambda \delta m^2)$ and $-2\lambda \delta m^2 \cos(2\lambda \delta m^2)$. Intersection of these two curves yield the maxima/minima in (b). The oscillations increase rapidly as E decreases, and are only sampled here at the bin points of these curves.

